Particle fluxes by subtropical pelagic communities under ocean alkalinity enhancement

Authors: Philipp Suessle[1], Jan Taucher[1], Silvan Goldenberg[1], Moritz Baumann[1], Kristian Spilling[2,3],
Andrea Noche-Ferreira[3,4], Mari Vanharanta[2,5], Ulf Riebesell[1]

Affiliations

[1] GEOMAR Helmholtz Centre for Ocean Research Kiel, Wischhofstrasse 1-3, 24148 Kiel, Germany

[2] Marine and Freshwater Solutions, Finnish Environment Institute, Helsinki, Finland

[3] Centre for Coastal Research, University of Agder, Kristiansand, Norway

[4] Department of Natural Sciences, University of Agder, Kristiansand, Norway

[5] Tvärminne Zoological Station, University of Helsinki, Hanko, Finland

Corresponding author: Philipp Suessle (psuessle@geomar.de)

Abstract

Ocean alkalinity enhancement (OAE) has been proposed as a carbon dioxide removal technology (CDR) allowing for long term storage of carbon dioxide in the ocean. By changing the carbonate speciation in seawater, OAE may potentially alter marine ecosystems with implications for the biological carbon pump. Using mesocosms in the subtropical North Atlantic, we

20 provide first empirical insights into impacts of carbonate-based OAE on the vertical flux and attenuation of sinking particles in an oligotrophic plankton community. We enhanced total alkalinity (TA) in increments of 300 µmol kg^{-1}, reaching up to ΔTA = 2400 µmol kg^{-1} compared to ambient TA. We applied a pCO$_2$-equilibrated OAE approach, i.e. dissolved inorganic carbon (DIC) was raised simultaneously with TA to maintain seawater pCO$_2$ in equilibrium with the atmosphere, thereby keeping perturbations of seawater carbonate chemistry moderate. The vertical flux of major elements including carbon,

25 nitrogen, phosphorus and silicon, as well as their stoichiometric ratios (e.g. carbon-to-nitrogen) remained unaffected over 29 days of OAE. The particle properties controlling the flux attenuation including sinking velocities and remineralization rates also remained unaffected by OAE. However, we observed abiotic mineral precipitation at high OAE levels (ΔTA = 1800 µmol kg^{-1} and higher) that resulted in a substantial increase in PIC formation. The associated consumption of alkalinity reduces the efficiency of CO$_2$ removal and emphasizes the importance of maintaining OAE within a carefully defined operating range.

30 Our findings suggest that carbon export by oligotrophic plankton communities is insensitive to OAE perturbations using a CO$_2$ pre-equilibrated approach. The integrity of ecosystem services is a prerequisite for large-scale application and should be further tested across a variety of nutrient-regimes and for less idealized OAE approaches.

Keywords: ocean alkalinity enhancement, carbon export flux, biological carbon pump, export flux stoichiometry,

35 remineralization, sinking velocities, climate change, nature-based solution

1 Introduction

Carbon dioxide removal (CDR) on a grand scale is likely to be needed to restrict global warming to between 1.5 to 2°C (IPCC, 2021). Oceans play a key role in buffering the climate by absorbing heat and CO_2 and ocean-based CDR could further enlarge
40   the oceanic carbon pool (GESAMP, 2019). Ocean alkalinity enhancement (OAE) has been proposed as one such measure (NAS, 2021). Simulating natural rock weathering, it elevates the oceans' total alkalinity (TA) by dissolving large amounts of minerals in seawater (Kheshgi, 1995; González and Ilyina, 2016). The associated change in carbonate speciation increases the capacity of seawater to take up CO_2 (Köhler et al., 2010; Hartmann et al., 2013). OAE has several potential benefits compared to other CDR technologies (Taylor et al., 2016). It does not compete for freshwater-, land-, or nutrient-use (Smith et al., 2016),
45   can rely on existing infrastructure from the mining industry (Renforth and Henderson, 2017), is applicable to large regions of the open ocean (Köhler et al., 2010) and additionally counters effects of ocean acidification (Doney et al., 2009; Gattuso et al., 2015). Different modelling studies suggest a potential CO_2 uptake by OAE ranging from $14 – 41$ Gt CO_2 year^{-1} (Paquay and Zeebe, 2013; González and Ilyina, 2016; Feng et al., 2017). For comparison, natural rock weathering currently locks up 1.1 Gt CO_2 year^{-1} (Ciais et al., 2014).
50   Before large scale deployment, the safety of OAE for marine organisms and ecosystem services has to be assured. OAE-related changes in pH, ion concentrations and the carbonate saturation state (Ω) would be permanent and may be elevated to well above current and pre-industrial levels (Feng et al., 2017; Renforth and Henderson, 2017). Such shifts in carbonate speciation might influence marine organisms (Bach et al., 2019a), analogous to effects observed for ocean acidification. In turn, calcifying organisms may theoretically benefit from alkalinity enhancement, as $CaCO_3$ precipitation is simplified allowing them to
55   allocate more energy towards growth or other metabolic processes (Jokiel, 2011; Monteiro et al., 2016; Bach, 2015). Riebesell et al. (2017) demonstrated that varying pH levels on natural communities caused large differences in population sizes of the prominent calcifying phytoplankton species *Emiliania huxleyi*. If there are ecological impacts of OAE, these would likely propagate through communities altering ecosystem services such as the biological carbon pump, which sequesters CO_2 into the deep ocean for hundreds to thousands of years (Boyd et al., 1999).
60   Several studies have revealed the influence of abiotic conditions on the magnitude and efficiency with which particulate organic carbon (POC) from photosynthetic biomass production is exported by gravitational settling (Schmittner et al., 2008; Taucher and Oschlies, 2011; Bopp et al., 2013; Martínez-García et al., 2014). Assuming a proliferation of calcifiers, organic carbon export could increase in response to higher carbonate ballasting (Honjo et al., 2008). Carbonate ballast is generally described by the fraction of particulate inorganic carbon (PIC) to particulate organic carbon (POC) (Klaas and Archer,
65   2002).The mineral's excess density (Francois et al., 2002) would increase sinking velocities (SV) of the export flux (Bach et al., 2016). With more carbonate ballasting, particles would on average sink deeper, thus storing atmospheric CO_2 for longer (Kwon et al., 2009). Additionally, particles containing $CaCO_3$ have shown reduced carbon remineralization rates (C_{remin}), possibly due to protection of POC in mineral shells, further increasing carbon transport to depth (Engel et al., 2009). A proliferation of calcifiers, however could also hamper OAE's capability to store atmospheric carbon (Bach et al., 2019a). The

70   CO_2 release associated with calcification is known as the carbonate counter pump and reflects a positive feedback on atmospheric carbon levels (Koeve, 2002; Salter et al., 2014). Recent laboratory-based OAE experiments (Moras et al., 2021; Hartmann et al., 2023) demonstrated an alkalinity consumption due to abiotic PIC precipitation, further highlighting its importance for larger scale OAE applications and implications on carbon export.

    The CO_2 sequestration potential of the biological pump also hinges on the stoichiometric ratios of carbon to other

75   macronutrients within the export flux (Shaffer, 1996; Schneider et al., 2003; Passow and Carlson, 2012). An OAE induced community restructuring could change the nitrogen-need per unit of exported carbon, binding the potential magnitude of carbon export to the supply of the limiting nutrient (Hessen et al., 2004). Such a change in carbon to particulate organic nitrogen ratios (POC:PON) has also been noted in response to changing heterotrophic processes under ocean acidification (Taucher et al., 2021), implying that similar effects might occur under OAE and further highlights the importance of stoichiometric ratios

80   for carbon sequestration. Whether or not OAE induces substantial changes in species communities and their mediation of the oceans natural carbon sequestration via the biological pump remains to be seen.

    Theoretically, OAE is conceivable in two different approaches. While one merely enhances alkalinity, letting CO_2 equilibrate with the atmosphere post application, the other approach entails adding solutions where CO_2 is already at equilibrium with the atmosphere, resulting in milder carbonate chemistry perturbations (so called pre-equilibrated approach). Here, we examined

85   influences of CO_2 pre-equilibrated, carbonate-based ocean alkalinity enhancement on drivers of the biological carbon pump. Using mesocosms in the subtropical North Atlantic, we examined whether OAE (with a doubling of the natural seawaters alkalinity) changes the magnitude and the stoichiometry of the carbon export flux, alters particle properties and if so, to what extent alkalinity consumption or enhanced ballasting through calcification occurs. With this first study on carbon export properties in a natural plankton assemblage, we provide urgently needed understanding on the biogeochemical side-effects of

90   OAE.

2 Material and Methods

2.1 Experimental setup

On the 8th of September 2021, nine in situ mesocosms were deployed in the harbor of Taliarte (27° 59′ 24″ N, 15° 22′ 8″ W;

95   east coast Gran Canaria, Spain). Each mesocosm was comprised of a 2.5 m long cylindrical polyurethane foil (Ø = 2 m) with a 1.5 m long conical sediment trap attached below. A polyethylene frame kept the mesocosm bags afloat and between sampling, mooring and pulley systems allowed to move the construction 2 m away from the pier, thereby reducing its influence on the light regime. The mesocosms were filled with seawater from ~100 m outside the harbor. Using a peristaltic pump, water from 2 – 10 m depth was filtered (< 3 mm) and gathered in an intermediate storage volume, from where each mesocosm

100   simultaneously received ~8 m³ in total. In order to reduce stress on the organisms, the speed of the peristaltic pump averaged ~17.35 L min⁻¹ and the entire process lasted ~7 h (for further technical details see Bach et al. (2019b)). Filling was done on the 10th of September and marks Day 0 of the experiment. OAE was simulated in a pCO$_2$-equilibrated OAE approach, meaning that dissolved inorganic carbon (DIC) was raised simultaneously with TA to maintain seawater pCO$_2$ in equilibrium with the atmosphere, thereby keeping perturbations of seawater carbonate chemistry (e.g. pH, Ω_{Ar}) as low as possible. This contrasts

105   non-equilibrated OAE, in which only TA would be increased (while DIC remains constant), leading to much larger transient changes in carbonate chemistry until seawater pCO$_2$ reaches equilibrium with the atmosphere due to air-sea gas exchange. Accordingly, a pre-equilibration of OAE solutions with CO$_2$ represent a least impactful, most optimistic OAE scenario. The OAE treatment in our mesocosm experiment was realized by adding CO$_2$-equilibrated solutions of sodium-carbonate and – bicarbonate (NaHCO$_3$/Na$_2$CO$_3$ in deionized water) on Day 4. With a custom-built device each 22 L solution was spread evenly

110   across the water column within 2.5 min. While one mesocosm was only treated with deionized water (control), the remaining eight received increments of ΔTA = 300 µmol kg⁻¹, resulting in 4689.3 µmol kg⁻¹ (Day 7) for the highest treatment level. This equaled double the alkalinity of the natural seawater. For details on changes in carbonate chemistry parameters see Table S1. The mooring of the mesocosms was randomized along the pier of the harbor and the experimental setup enabled us to monitor pelagic communities and biogeochemical responses to OAE for 29 days.

115

Table 1 | Experimental design displaying the increments of TA increase relative to the natural background alkalinity of 2402.7 µmol kg⁻¹

OAE (ΔTA µmol kg⁻¹)	0	300	600	900	1200	1500	1800	2100	2400
Symbol	▲	●	■	◆	▼	●	■	◆	▲

2.2 Sampling procedure and maintenance

In general, sampling was done every 2 days between 09:00 and 12:00 a.m. Additionally, to follow any biological responses
related to the filling process, daily sampling was conducted prior to the alkalinity addition. Bulk water samples were taken
with a polypropylene pipe, integrating the upper 2.3 m of the water column. On each sampling occasion, 40 – 60 L (8 – 12
tubes) of water were sampled per mesocosm. The water was stored dark and at in-situ temperature in several carboys and
transported back to the lab-facilities for analysis of chlorophyll a (Chl a), TA and dissolved inorganic carbon (DIC), dissolved
inorganic nutrients ($NO_3^- + NO_2^-$, PO_4^{3-}, $Si(OH)_4$), as well as water column particulate matter (PM_{WC}). Other measurements
conducted during the study included analysis of primary productivity, photosynthetic pigment analysis, phyto- and
microzooplankton analysis and prokaryotic heterotrophic production. A CTD60M (Sea & Sun Technology GmbH,
Trappenkamp, Germany) was cast for additional abiotic parameters such as temperature, salinity, pH, turbidity, oxygen (O_2)
and photosynthetically active radiation. Particulate matter from the sediment trap (PM_{ST}) was collected using a manual vacuum
pump, not exceeding 0.3 bar during the pumping. Stored in 5 L glass bottles (Schott Scandinavia A/S, Kgs. Lyngby, Denmark),
the sediment was kept dark until further processing in the lab (see Boxhammer et al. (2016) for technical details). Homogenous
subsamples were taken after resuspension of the sediment by gentle rotation of the glass bottles. The subsamples were used
for determination of carbon-specific remineralization rates (C_{remin}) and particle sinking velocities (SV) as described below.

The inside of the mesocosm walls was cleaned every 4 to 6 days with brushes to prevent nutrient consumption and shading
from organisms growing on the walls (for a detailed experimental schedule see Paul et al. 2023). To further counteract shading,
cleaning from the outside was done three times during the experiment by divers equipped with brushes. During cleaning on
Day 16, the sediment hose of mesocosm ΔTA_{900} detached. Pumping PM_{ST} on the subsequent sampling day was not possible,
thus SV measurements on Day 17 are missing for this mesocosm. Measurements of SV and C_{remin} on Day 19 however are not
discarded, as they did not significantly differ from other treatment levels on that day. Yet, interpretation should be done with
care, as the period for PM_{ST} settlement was ~5 h less than usual.

2.3 Drivers of the biological carbon pump

2.3.1 Export fluxes and stoichiometry

PM_{ST} material was prepared for analysis of total particulate carbon and nitrogen (TPC/N_{ST}), particulate organic carbon,
nitrogen and phosphorus (POC/N/P_{ST}) as well as biogenic silica (BSi_{ST}) after subsampling. First of all, particles were separated
from the seawater. To increase flocculation and coagulation, 3 mol L^{-1} ferric chloride ($FeCl_3$) were therefore added to the 5 L
bottles with sediment material, followed by the addition of 3 mol L^{-1} NaOH to counteract the decreasing pH (Boxhammer et
al., 2016). After 1 h of settlement, the supernatant was decanted and the remaining flocculated material was centrifuged for 10
min at 5.200 g in a 6–16KS centrifuge (Sigma Laborzentrifugen GmbH, Osterode am Harz, Germany). A second centrifugation
step for 10 min at 5.000 g in a 3K12 centrifuge (Sigma) yielded solid sediment pellets. The pellets were stored at -20°C and
transported back to Kiel for further processing. At GEOMAR, samples were freeze-dried to remove remaining moisture and

150 ground to a fine homogenous powder in a cell mill (Edmund Bühler GmbH, Bodelshausen, Germany). The sediment powder was stored dark and cool in glass or plastic vials until further processing. Sediment powder was transferred into silver or respectively tin capsules, and either acidified with 1 mol L^{-1} HCl and dried at 50°C over-night in order to measure POC/N$_{ST}$, or proceeded unacidified for TPC/N$_{ST}$ analysis. Duplicates were measured on a CN analyzer (Euro EA-CN, HEKAtech GmbH, Wegberg, Germany) according to (Sharp, 1974). PIC$_{ST}$ concentrations were calculated from the difference of TPC$_{ST}$ to POC$_{ST}$.

155 BSi$_{ST}$ and POP$_{ST}$ concentrations were measured spectrophotometrically according to Hansen and Koroleff (1999), after subsampling ~ 2 mg of the sediment. Prior to that, POP samples were pressure-cooked in 40 ml of deionized water including an oxidizing agent (Oxisolv, Merck).

2.3.2 Particle sinking velocities

Sinking velocities (SV) of sediment trap material were determined every two days by means of video-microscopy. A
160 repurposed FlowCam (Fluid Imaging Technologies Inc., Scarborough, United States) was used to capture images of particles during gravitational sinking. A vertically mounted sinking chamber (cuvette with the dimensions 10 x 10 x 350 mm) was placed in front of the camera (see Bach et al. (2012) for technical details). Sediment subsamples were inspected visually and diluted (with filtered seawater < 0.2 µm) in a small cup according to their particle density (1:1 – 1:40). Diluted samples were loaded into the sinking chamber by a pipette and pileus ball attached atop. Fluid advection within the sinking chamber could
165 be ruled out by ensuring air-tightness. Measurements were carried out at in situ temperatures (~22°C) and additional ventilation minimized convection within the sinking chamber. Particles between 25 – 1000 µm were identified with a 2x magnification and 20 frames-per-second, and their sinking velocities were calculated by applying a linear regression to the vertical position against time. Several optical parameters allowed to identify the multiple frames of a single particle during gravitational sinking and calculations in the MATLAB script (version R2021b; provided by Bach et al. (2012), see "Evaluation of sinking
170 velocities") were adjusted to the more recent version of the FlowCam 8000. These were corrected for temperature differences during measurements and for wall effects of the sinking chamber following Ristow (1997). Partially captured particles, or those out of focus were excluded within the MATLAB script, prior to the SV calculation. Measurements were run for 20 min and subsequent data analysis was carried out with the programming software R (R Core Team, 2021) using the package *tidyverse* (Wickham et al., 2019) in RStudio (Version 4.1.1.). It is important to note that measured particle size spectra are
175 derived from ex situ measurements and thus do not accurately represent the in situ size distribution. Nevertheless, they allowed to follow in situ particle dynamics due to e.g., aggregation, packing or grazing closely.

2.3.3 Remineralization rates of sinking particles

Carbon specific remineralization rates were determined every 4 – 6 days. During the water column sampling, four replicate and three control bottles for each mesocosm were filled headspace-free. Upon arrival in the temperature-controlled lab (in situ
180 temperature of the respective day), the respiration bottles were acclimatized in a water bath for 1 h. Depending on particle density, 0.5 – 10 ml of homogenized sediment subsample of the respective mesocosm were slowly injected into four replicated

bottles. Control bottles (n = 3) did not receive any sediments. Subsequently, all bottles were dark-incubated on a plankton wheel (~1 rpm) for 22 – 26 h. Non-invasive O_2 measurements were carried out in regular intervals (appr. every 4 h) using a fiber optical measurement device (Fibox4 Trace, PreSens – Precision Sensing GmbH, Regensburg, Germany) and PSt3 sensor

185   spots (PreSens) mounted to the inside walls of the incubated bottles. Corrections for atmospheric pressure and temperature (using a dummy bottle) were automatically done by the Fibox4. The Fibox4 salinity correction was set to the mean mesocosm salinity of the respective day (CTD measurement).

Incubations were terminated with the collection of POC (sediment + suspended) within the bottles on pre-combusted glass fiber filters (0.7 µm, Whatman). The carbon content analysis was carried out as described for POC_{WC} (see Sect. 2.3.4). The

190   carbon specific remineralization rate of sedimented particulate matter (C_{remin} in d^{-1}) was calculated as follows:

$$C_{remin} = \frac{(r * RQ)}{(POC + r * RQ * \Delta t)} \tag{1}$$

The O_2 consumption rate (r in µmol O_2 L^{-1} d^{-1}) was normalized to the POC (µmol C L^{-1}) contained within the bottles, which was corrected for the duration of the incubation (Δt in d). The respiration quotient (RQ in mol C mol O_2^{-1}) equalled 1, since

195   the consumption of O_2 is commonly assumed to be equal to the production of CO_2 during organic matter turnover (Ploug and Grossart, 2000; Iversen and Ploug, 2013; Bach et al., 2019c). To differentiate the influence of sediment respiration from ambient seawater O_2 consumption, C_{remin} was corrected for the mean blank bottle values.

2.3.4 Phytoplankton biomass and water column stoichiometry

Subsampling for TPC/N_{WC}, POC/N_{WC} and Chl a was achieved by filtering the water column samples onto separate pre-

200   combusted glass fiber filters (0.7 µm, Whatman). To remove inorganic carbon, POC/N_{WC} filters were acidified for ~30 sec. using 1 mol L^{-1} HCl. Additionally, unacidified filters for TPC/N_{WC} were collected. Both filter types were stored in pre-combusted glass petri-dishes and dried at 60°C overnight. All filters were packed into tin-cups (8 x 8 x 15 mm, LabNeed GmbH, Nidderau, Germany), stored in a desiccator and transported back to Kiel. Carbon content of filters was determined with a CN analyzer (Euro EA-CN, HEKAtech) as described for the sediment trap samples. PIC_{WC} concentrations were

205   calculated as described for the sediment trap samples.

Chl a was extracted in plastic vials using acetone (90%) and subsequent homogenization in a cell mill with glass beads (5 min; Vibrogen, Berlin, Germany). The suspension was centrifuged (10 min, 800 g, 4°C; Universal 320, Hettich, Bäch, Germany) and the resulting supernatant was analyzed with a fluorometer (TURNER Trilogy, Turnerdesigns, San Jose, United States) according to Welschmeyer (1994). Spinach Chl a extract (Sigma-Aldrich, St. Louis, United States) was used to calibrate the

210   fluorometer (Strickland and Parsons, 1972).

2.3.5 Carbonate chemistry and nutrient concentrations

TA and DIC samples were taken with an overflow of ~2 times the final sampling volume, carefully avoiding air-inclusion. Within 12 h, samples were measured at room temperature. To remove PIC_{WC}, both TA and DIC samples were filtered (0.2 µm, Whatman). TA was determined in duplicates with hydrochloric acid (0.05 M) in a two-stage open cell potentiometric
215 titrator (Compact Titrosampler 862, Metrohm, Munich, Germany).

DIC was determined in triplicates by infrared absorption using an AIRICA system (MARIANDA, Kiel, Germany) with a differential gas analyzer (LI-7000, LI-COR Biosciences GmbH, Bad Homburg, Germany). Values of DIC and TA were calibrated against certified reference material (batch no.: 143, 190; Dickson, 2010). Further carbonate chemistry parameters were calculated with the excel macro "*CO2SYS*" (Pierrot et al., 2011) using the (water column averaged) temperature and
220 salinity CTD measurements for correction. The carbonate dissociation constants (K_1 and K_2) from Lueker et al. (2000) were chosen.

Dissolved inorganic nutrient concentrations ($NO_3^- + NO_2^-$, PO_4^{3-}, $Si(OH)_4$), were measured spectrophotometrically on a five channel continuous flow analyzer (QuAAtro AutoAnalyzer, SEAL Analytical Inc., Mequon, United States) with a fluorescence detector (FP-2020, JASCO, Pfungstadt, Germany). Approaches of Murphy and Riley (1962), Mullin and Riley (1955) and
225 Morris and Riley (1963) were followed for all colorimetric methods and refractive index correction was done according to Coverly et al. (2012).

2.3.6 Statistical analysis

Linear mixed effects models were used to assess the OAE effect on the different export-related response variables. OAE was employed as continuous and Day as categorical fixed effect and Mesocosm as random effect (*nlme* package; Pinheiro et al.,
230 2020). The interaction term of OAE × Day was employed as additional fixed effect to test how the OAE effect changed over time. For all analyses, assumptions were checked using residual-vs-fitted plots (homogeneity of variances and QQ Plots (normality of residuals; *performance* package; Lüdecke et al., 2021). Their violation was corrected for with data transformations (Table S3). All analyses were conducted at a significance level of α = 0.05 using R (R Core Team, 2021). Additionally, averages over experimental phases were calculated for specific response variables and their dependency on OAE
235 tested using simple linear regressions. The highest OAE level (ΔTA_{2400}) was excluded from all statistical analyses as it developed considerable abiotic precipitation which interfered with the interpretation of the OAEs effect on the biological pump. A *Welch´s t-test* on TA between two phases of the experiment (Day 4 – 17 vs. Day 19 – 33, Table S2) confirmed its standing as an extreme outlier.

3 Results

3.1 Achieved alkalinity enhancement and plankton community biomass

We successfully applied OAE to the mesocosms and target alkalinity levels remained stable throughout the experiment (Fig. 1a). An exception was the highest OAE level, which only remained stable until Day 17, after which ΔTA_{2400} continuously declined, dropping below ΔTA_{2100} on Day 33. This alkalinity consumption was induced by abiotic calcium carbonate precipitation (see Sect. 4.2). Phytoplankton biomass approximated by chlorophyll a and particulate organic carbon in the water column (POC_{WC}) did not change with respect to OAE (Fig. 1b,c, Table S4). It remained low in the first half of the experiment (Day 3 – 21 Fig. S3), where after phytoplankton biomass unexpectedly increased in some mesocosms (ΔTA_{600}, ΔTA_{900}, ΔTA_{1500}, and ΔTA_{1800}). These blooms occurred despite oligotrophic conditions throughout the entire experiment (Fig. S2) and were likely driven by regenerated nitrogen sources, such as ammonium (Paul et al. in preparation).
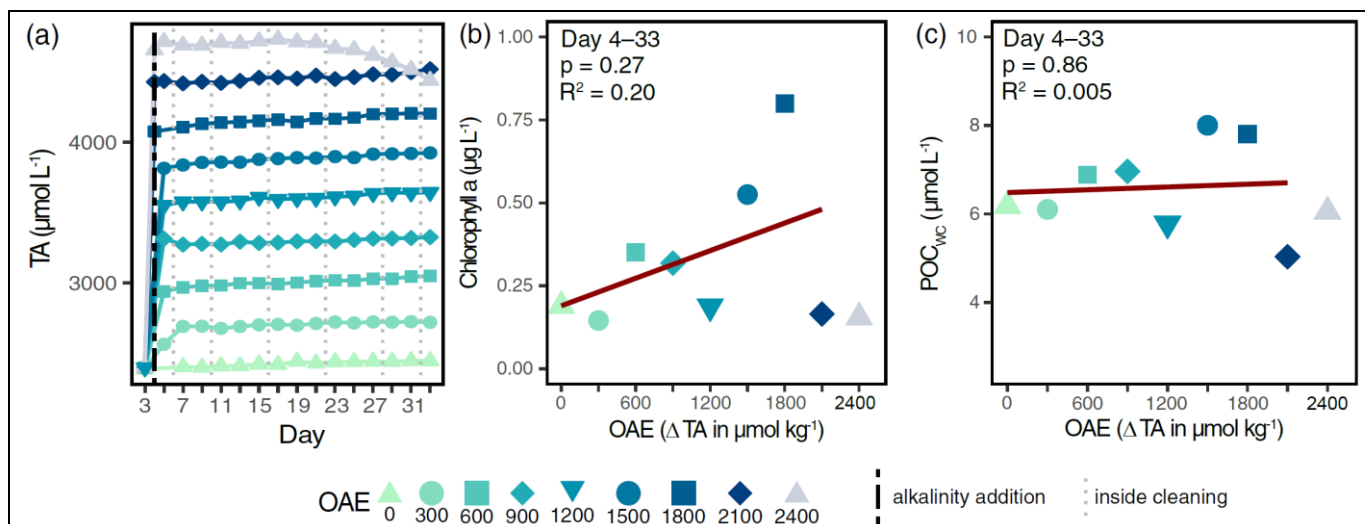
Figure 1| Abiotic and biotic responses of the water column to the application of OAE. Achieved alkalinity enhancement and its stability over time (a). The vertical black line indicates the alkalinity addition and the grey lines the inside cleaning of the mesocosm walls. Chlorophyll a (b) and carbon biomass (c) of the plankton community. Averages over the treatment period are employed in linear regressions.

3.2 Organic matter fluxes and stoichiometry

Ocean alkalinity enhancement did not influence the magnitude of the particulate organic carbon flux (POC_{ST}), neither the cumulated POC_{ST} over the entire experiment, nor on a daily basis (Table S3a). Irrespective of OAE, carbon export fluxes decreased over time (Fig. 2a). Higher initial fluxes (Day 7 & 9) reflected the decreasing phytoplankton biomass of preceding days and thereupon, an average 8-fold decrease was visible until day 27. Other major elemental fluxes (PON_{ST}, POP_{ST} and BSi_{ST}) were likewise not influenced by OAE (Fig. 2c,e,f, Table S3i,j,k) and had similar temporal trends as POC fluxes (Fig. S4b,c,d). Whether the export of the major elements was affected within the blooming mesocosms (ΔTA_{600}, ΔTA_{900}, ΔTA_{1500}, and ΔTA_{1800}, Fig. S4) remains unclear, yet the influence of wall cleaning is apparent from Day 17 onwards, as wall growth intensified. Carbon-to-nitrogen ratios ($POC_{ST}:PON_{ST}$) of exported matter did not change with respect to OAE (Fig. 2d). The stoichiometric composition stayed constant throughout the experiment (Table S3b) and generally well above the canonical Redfield ratio of 6.6 (Fig. S4a). Likewise, opal ballasting ($BSi_{ST}:POC_{ST}$) was unaffected by OAE (Fig. 2g, Fig. S4e, Table S3l).
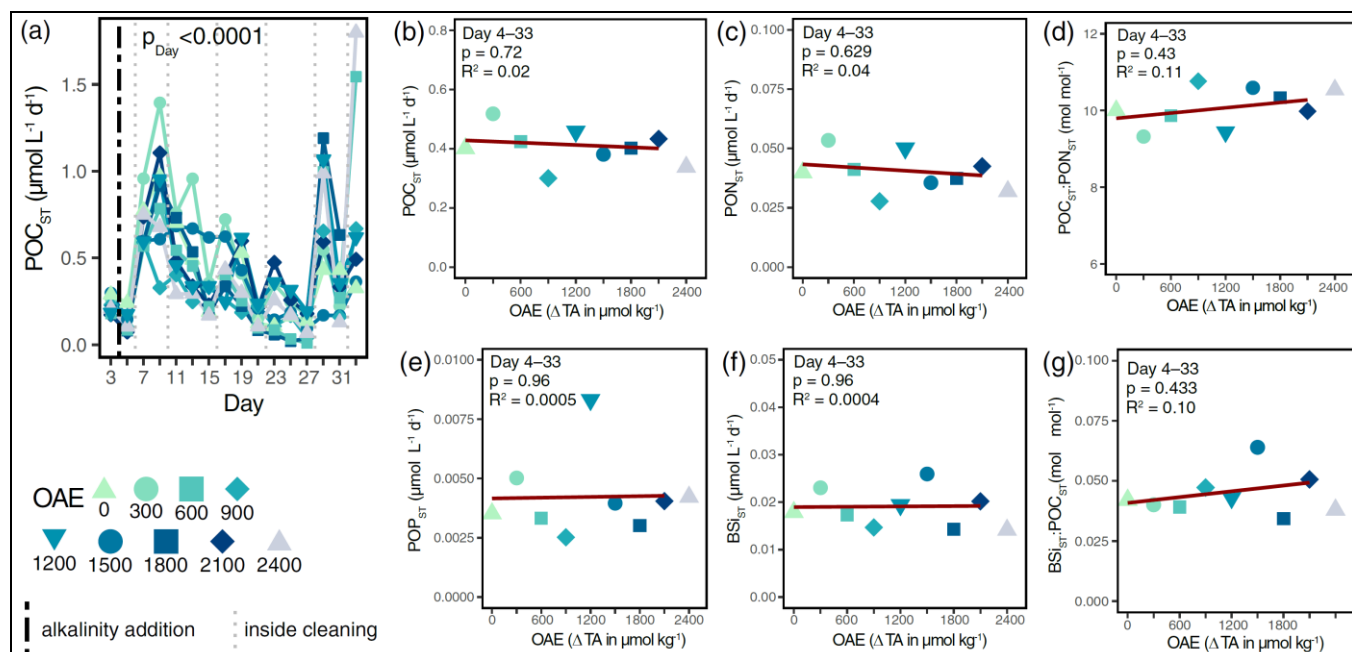
Figure 2| Organic matter fluxes and stoichiometry under the application of OAE. Organic carbon flux and its response to OAE over time (a) and averaged across the treatment period (b). The p-value in (a) represents the output of linear mixed effects model (Table S3a). The vertical black line indicates the alkalinity addition and the grey lines the inside cleaning of the mesocosm walls. Other major elemental fluxes (PON_{ST}, POP_{ST}, BSi_{ST}) in response to OAE averaged over the treatment period (c,e,f). Quality and ballasting of the export flux ($POC_{ST}:PON_{ST}$, $BSi_{ST}:POC_{ST}$) averaged over the treatment period employed as linear regressions (d, g).

3.3 Particle sinking velocities and remineralization rates

275   OAE had no effect on either particle sinking velocities or remineralization rates of sinking material, leaving the potential flux attenuation with depth unchanged (Fig. 3a, c and Table S3f,m). Particle sinking velocities (SV) were generally low ($10 - 35$ m d^{-1}) and did not respond to OAE, neither overall (Fig. 3a), nor for specific particle size classes (Fig. S5). Sinking velocities of ΔTA_{2400} exceeded those of all other alkalinity levels from Day 15 onwards and are expected to be caused by increased ballasting due to the abiotically precipitated carbonate mineral (see Sect. 4.2). Remineralization rates (C_{remin}) did not change

280   under OAE (Fig. 3c, Table S3f), staying relatively constant with carbon turnover varying between 7 and 18% per day (Fig. 3c). Noticeably higher remineralization rates of ΔTA_{2400} on Day 27 and 33 were not paralleled by higher O_2 consumption rates across incubations (Fig. S7) and were probably caused by an unresolved sample processing error due to the abiotic precipitation (see Sect. 4.2).
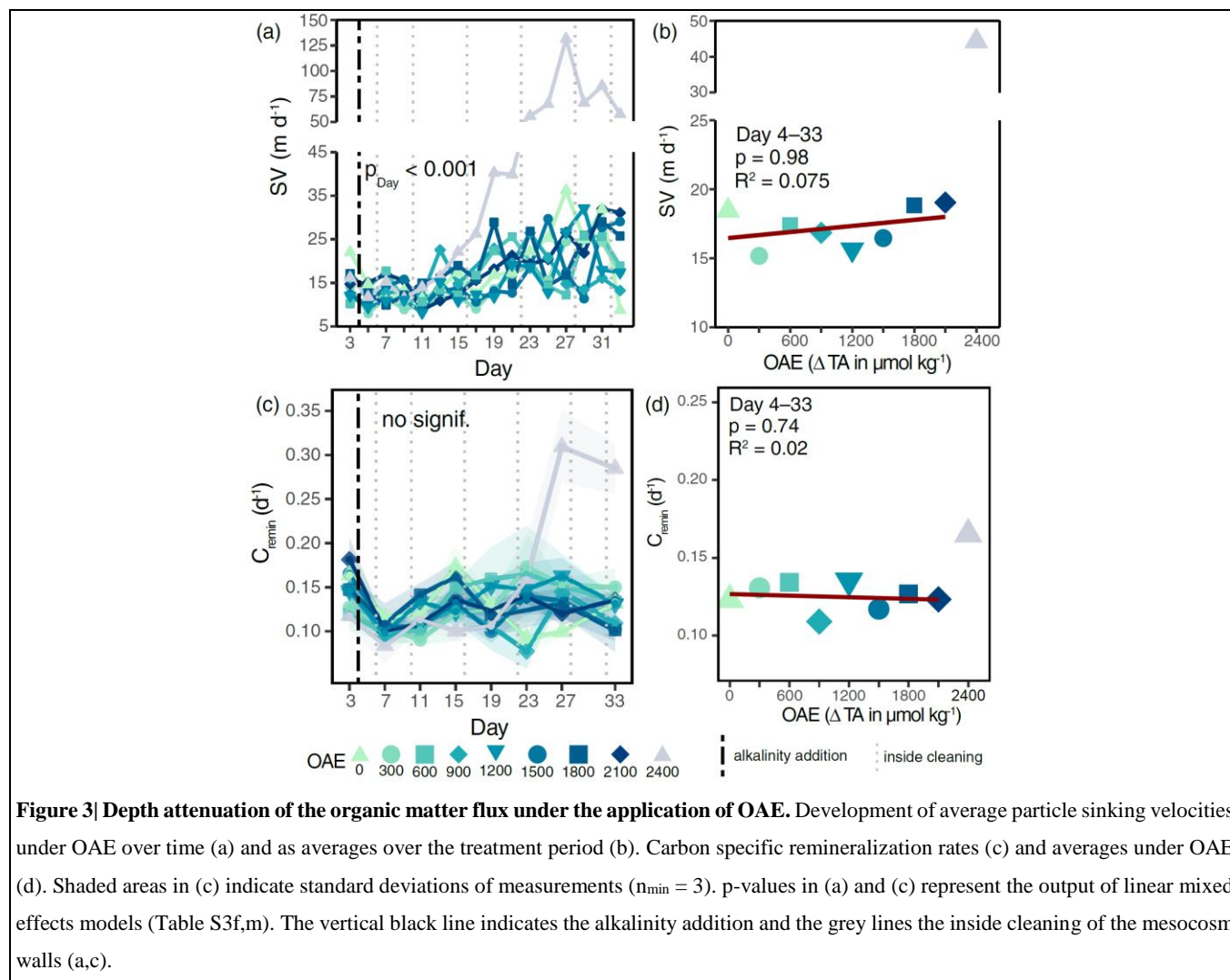
285   **Figure 3| Depth attenuation of the organic matter flux under the application of OAE.** Development of average particle sinking velocities under OAE over time (a) and as averages over the treatment period (b). Carbon specific remineralization rates (c) and averages under OAE (d). Shaded areas in (c) indicate standard deviations of measurements ($n_{min} = 3$). p-values in (a) and (c) represent the output of linear mixed effects models (Table S3f,m). The vertical black line indicates the alkalinity addition and the grey lines the inside cleaning of the mesocosm walls (a,c).

3.4 Abiotic precipitation, inorganic carbon fluxes and carbonate ballasting

290

Particulate inorganic carbon export (PIC_{ST}) and carbonate ballasting (PIC_{ST}:POC_{ST}) increased under OAE (Fig. 4a, Fig. S6a, Table S3g,h). Between Days 19 and 31, average PIC_{ST} fluxes almost tripled from ambient seawater alkalinity to ΔTA_{2100} (Fig. 4b), while carbonate ballasting more than doubled (Fig. S6b). Additionally, the PIC_{ST} flux in ΔTA_{2400} exceeded those of all other alkalinity levels from Day 17 onwards and pCO$_2$ was highest (e.g., 541 µatm on Day 33). High PIC_{ST} fluxes coincided

295 with a white precipitate (Fig. S8d), especially apparent on the walls of the mesocosm ΔTA_{2400}, which upon wall cleaning sank to the sediment traps. This direct consequence of the abiotic precipitation increased ballasting material within the sediment trap and thus particle sinking velocities (Fig. 4c). Sinking velocities in the medium (100 – 250 µm) particle size class increased by 30 m d^{-1} with every mol mol^{-1} in PIC_{ST}:POC_{ST}. Although less discernible, particles in the smallest size range (25 – 100 µm) increased by 18.10 m d^{-1} per increment of PIC_{ST}:POC_{ST} (note marginally significance: $p = 0.065$, Table S4). While screen-

300 captures from the FlowCam indicated, that larger particles were actually ballasted (distinct and dark particles in aggregates, Fig. 4d), solitary precipitates were also visible. It appears that both, ballasting of larger aggregates within the sediment trap and solitary precipitates increased the measured particle sinking velocities across all sizes (Fig. S5).
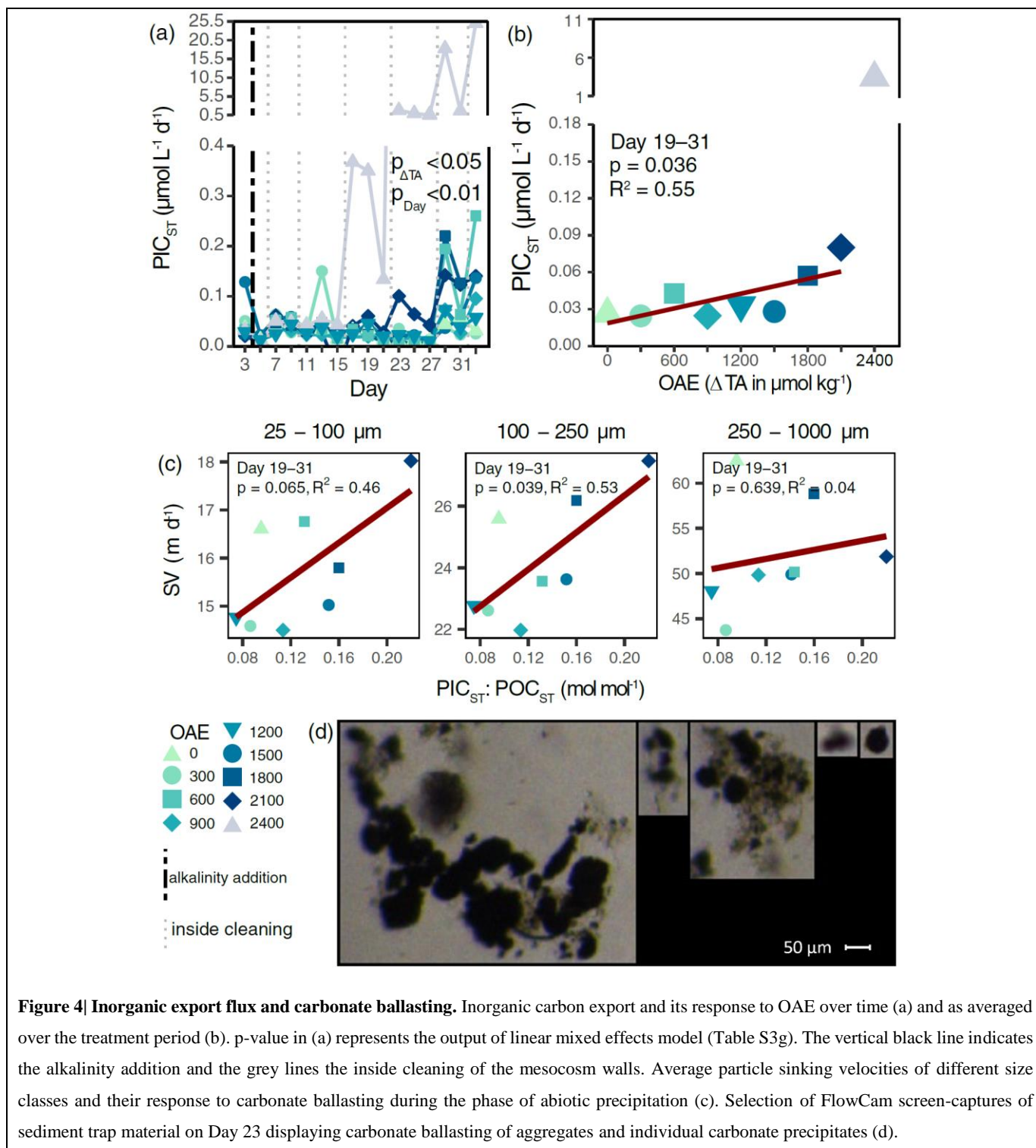
Figure 4| Inorganic export flux and carbonate ballasting. Inorganic carbon export and its response to OAE over time (a) and as averaged over the treatment period (b). p-value in (a) represents the output of linear mixed effects model (Table S3g). The vertical black line indicates the alkalinity addition and the grey lines the inside cleaning of the mesocosm walls. Average particle sinking velocities of different size classes and their response to carbonate ballasting during the phase of abiotic precipitation (c). Selection of FlowCam screen-captures of sediment trap material on Day 23 displaying carbonate ballasting of aggregates and individual carbonate precipitates (d).

4 Discussion

4.1 Particle export by the plankton community

Ocean alkalinity enhancement did not influence the biotically driven flux of major elements (C, N, P, Si), stoichiometric ratios or potential depth attenuation (particle sinking velocities and remineralization rates). These findings are in line with the lack of a detectable effect on plankton community composition or water column biogeochemistry during our experiment (Paul et al. in preparation). Theoretically expected responses of calcifiers to OAE (due to an increase in Ω_{Ar}) were either absent or not detected due to their low abundances (Fig. S8a-c). We worked in a nutrient deprived ecosystem and simulated pCO$_2$-equilibrated OAE, only changing pH by up to 0.2 units. The absence of consistent blooms and the deliberately small carbonate chemistry perturbations allowed us to assess this least impactful OAE scenario, which apparently did not influence plankton communities and the elemental fluxes they drive. This is consistent with previous ocean acidification studies, which found pronounced responses only at larger pH differences and during blooms (Stange et al., 2018; Taucher et al., 2017). Therein, particle fluxes only changed for a pH decrease of 0.5 units and upon adding nutrient-rich deep water to the oligotrophic system, which stimulated considerable primary production, in contrast to our study. While there is a chance that OAE effects might have emerged with longer experiment duration, added alkalinity for different application scenarios (e.g., in wake of ships) is expected to dilute on time scales considerably shorter than our study-length (Byrne et al., 1988). This gives further confidence that the particle fluxes, their properties and therefore the potential to sequester carbon via the biological pump would remain unimpeded in the oligotrophic open ocean under CO$_2$ pre-equilibrated OAE.

Other approaches, however, let pCO$_2$ equilibrate post alkalinity application and might be conducted in nutrient-rich ecosystems. Carbonate chemistry perturbations thus can be more severe during OAE and responses of plankton communities thereto might even be amplified during blooms, ultimately altering the biological carbon pump. For instance, non-equilibrated OAE could lead to CO$_2$ limitation in phytoplankton, which could hamper primary and subsequently biomass production (Bach et al., 2020; Zagarese et al., 2021; Riebesell et al., 1993) with the potential to decrease export production. Non-equilibrated alkalinity enhancement also entails a stronger pH change at which effects absent at milder perturbations might eventually emerge, analogous to several ocean acidification studies (Stange et al., 2018; Taucher et al., 2017). A lesson from strong pH perturbations under ocean acidification is that bacterial activity might increase (Piontek et al., 2010; Endres et al., 2014), such that a decrease under non-equilibrated OAE is conceivable. This would impair nutrient recycling and release in the surface ocean (Karthäuser et al., 2021; Cabanes et al., 2017), eventually shortening the bloom period (Böckmann et al., 2021; Sarthou et al., 2008; Cherabier and Ferrière, 2022) and consequently decrease the potential export production throughout a season (Iversen, 2023). On the other hand, copepods have been shown to increase their feeding rates in response to elevated pH (Li et al., 2008). Increased in- and egestion rates are thus conceivable under OAE, potentially leading to a larger amount of fast sinking fecal pellets (Stukel et al., 2011; Le Moigne et al., 2016), which eventually would decrease the depth attenuation of the export flux (Guidi et al., 2015).

While oligotrophic conditions in the Canary Island region are prevailing, eddy-induced nutrient upwelling is not uncommon (Arístegui et al., 1997; Basterretxea et al., 2002). Additionally, application of OAE is also considered in nutrient-rich coastal

345 zones or upwelling areas, since it would require less technical efforts compared to open ocean applications, as represented by our study (Bach et al., 2019a). Thus, alkalinity enhanced water parcels may experience blooms. In parallel to several ocean acidification studies the blooming communities' sensitivity towards the concomitant carbonate chemistry perturbations can alter particle fluxes and emissions of climate relevant trace gases (Bach et al., 2016; Webb et al., 2016; Riebesell et al., 2017; Stange et al., 2018; Taucher et al., 2017). Thus, feedbacks of OAE on the biological carbon pump may be diverse, necessitating

350 research on different application approaches and across nutrient regimes in further multi-trophic ecosystem studies.

4.2 Abiotic precipitation and alkalinity leakage

Particulate inorganic carbon fluxes increased with alkalinity enhancement; an effect that became more prominent with time. Yet, observed fluxes were apparently not driven from biotic production, given the low abundances of calcifying organisms during our mesocosm experiment (Xin et al. in preparation; Fig. S8). Instead, the increased carbonate fluxes and the alkalinity

355 loss observed in ΔTA_{2400} resulted from abiotic precipitation. This process was not unique to the highest treatment, as carbonate fluxes and water column ballasting ratios increased at lower treatment levels (ΔTA_{1800} and ΔTA_{2100}) as well (Paul et al. in preparation).

Such abiotic precipitation under OAE has been observed previously (Moras et al., 2022; Griffioen, 2017; Subhas et al., 2022) and is known to occur for carbonate saturation states well below the threshold for spontaneous precipitation (Table S1

360 compared to Ω_{Ar} = 12.5-13.5, Morse and He, 1993). In fact, Wurgaft et al. (2021) noted carbonate precipitation at alkalinity concentrations close to our control treatment. The process can be initiated by the presence of suitable precipitation nuclei which has been noted in the field (Wurgaft et al., 2021) and during separate short-term incubations with mesocosm water during our campaign (Hartmann et al., 2023). Artificial surfaces for precipitation were present through the mesocosm walls, which in combination with the perturbed carbonate chemistry may explain the observed precipitation at our higher alkalinity

365 levels. Thus, a large portion of the formed PIC could be regarded an experimental artefact, which needs to be considered, when interpreting particle sinking velocities. The majority of precipitated carbonates slid down the mesocosm walls upon cleaning, so that most ballasting likely occurred through aggregation within the sediment trap where both PIC from the walls and POC from the water column accumulated. Given this spatial separation of inorganic and organic carbon flux production, it seems improbable that significant ballasting of aggregates occurred through scavenging of particles within the water column.

370 Therefore, abiotic precipitation likely did not affect sinking velocities in the water column such that the increase over time could not have actually affected the potential depth attenuation of the biological pump during our experiment. Additionally, the magnitude of PIC formation in open ocean settings would likely be substantially lower than during our study, since suitable precipitation nuclei are mostly scarce.

375   Abiotic precipitation, however has also been noted for suspended particles (Ferderer et al., 2022; Hartmann et al. 2023). It is thus not only imaginable for coastal ecosystems with large surface areas (e.g., seagrass meadows), but also for the open ocean, given the periodically presence of precipitation nuclei through e.g., dust deposition. Although OAE should be maintained well outside a TA range where such precipitation might occur, it is worthwhile to consider its potential implications on particle fluxes should such a worst-case scenario arise. Carbonate ballasting from OAE-induced precipitates is likely to behave

380   differently, as compared to e.g., coccolithophore-derived ballasting. Opposing to abiotic precipitates, biological carbonate-containing particles also include lighter organic matter, which exert less ballast on sinking aggregates. In addition, the abiotic PIC particles were considerably larger (50 µm) than e.g. coccolithophore-derived particles (Jordan, 2009; Rothwell, 2016). Larger particles have been shown to be scavenged and ballast sinking aggregates preferably (Puig et al., 2013; McCave, 1983). Abiotic precipitates are thus not only heavier at similar size, but potentially also larger, exerting more ballasting potential than

385   many biologically derived carbonates and may substantially alter open ocean export dynamics under such adverse OAE scenarios. The onset of abiotic carbonate precipitation would also oppose the desired effects of ocean alkalinity. Given the supersaturation of surface waters with respect to calcium carbonate (Mucci, 1983), a significant export of the precipitated carbonate mineral is conceivable, transporting alkalinity to waters out of contact with the atmosphere. Such calcium carbonate precipitation releases CO_2 (Zeebe and Wolf-Gladrow, 2010), further decreasing OAE's efficacy to store atmospheric carbon.

390   Additionally, abiotic carbonate precipitation may sustain itself to a point were alkalinity drops below initial background concentrations (Moras et al., 2022; Brečević and Nielsen, 1989; Hartmann et al., 2023), eventually turning alkalinity enhanced waters into a source, rather than a sink for CO_2.

5 Conclusions

Our findings suggest that particle fluxes by subtropical pelagic communities are insensitive to CO_2 pre-equilibrated OAE,

395   leaving carbon sequestration via the biological pump unimpeded by this most optimistic approach. It will be paramount to test effects on the magnitude and quality of export fluxes across nutrient-richer ecosystems and for non-equilibrated OAE approaches. Undesired abiotic carbonate precipitation may induce alkalinity consumption and requires close monitoring. It may not only decrease OAE`s efficacy to store atmospheric carbon, but potentially also alters the biological pump`s capability to sequester atmospheric CO_2. Ultimately, our results are a promising starting point for further assessments on this carbon

400   dioxide removal technology, prompting the necessity to holistically consider biotic and abiotic impacts, before drawing sound conclusions on the safe applicability of OAE.

Acknowledgements

405   The authors would like to thank the Oceanic Platform of the Canary Islands (PLOCAN) and its staff for the use of their facilities and for their help with the logistics and organisation of this experiment. We would also like to express our gratitude towards Andrea Ludwig, Jana Meyer, Jan Hennke, and Anton Theileis for logistical and technical support during and before our study. Further, we are thankful for the help of the KOSMOS Scientific Diving and Maintenance Team, Michael Sswat, Carsten Spisla, Daniel Brüggemann, Silvan Goldenberg, Joaquin Ortiz, Nicolás Sánchez. Additionally, we would like to thank Levka Hansen
410   and Kerstin Nachtigall for laboratory support in Kiel and at last Anna Groen, Juliane Tammen and Julietta Schneider for further laboratory work and sample analysis, both on-site and in Kiel. We would also like to thank the Finnish marine research infrastructure (FINMARI) for providing relevant equipment to conduct our measurements.

Data availability

The raw data supporting the conclusions of this article will be made available by the authors as soon as possible.

415   **Author contribution statement**

Study design and conceptualisation: PS, JT, SG, MB, UR

Sampling and laboratory analysis: PS, AN, MV, KS

Data analysis and interpretation: PS, MB, SG, JT, UR

Writing – original draft: PS

420   Writing – reviewing and editing: all authors

Funding

This study was funded by the OceanNETS project ("Ocean-based Negative Emissions Technologies – analysing the feasibility, risks and co-benefits of ocean-based negative emission technologies for stabilizing the climate", EU Horizon 2020 Research and Innovation Programme Grant Agreement No.: 869357), and the Helmholtz European Partnering project Ocean-CDR
425   ("Ocean-based carbon dioxide removal strategies", Project No.: PIE-0021) with additional support from the AQUACOSM-plus project (EU H2020-INFRAIA Project No.: 871081, "AQUACOSM-plus: Network of Leading European AQUAtic MesoCOSM Facilities Connecting Rivers, Lakes, Estuaries and Oceans in Europe and beyond").

Competing interests

The contact author has declared that none of the authors has any competing interests.

430 **References**

Bach, L. T.: Reconsidering the role of carbonate ion concentration in calcification by marine organisms, Biogeosciences, 12, 4939–4951, https://doi.org/10.5194/bg-12-4939-2015, 2015.

Bach, L. T., Riebesell, U., Sett, S., Febiri, S., Rzepka, P., and Schulz, K. G.: An approach for particle sinking velocity measurements in the 3–400 μm size range and considerations on the effect of temperature on sinking rates, Mar Biol, 159,
435 1853–1864, https://doi.org/10.1007/s00227-012-1945-2, 2012.

Bach, L. T., Boxhammer, T., Larsen, A., Hildebrandt, N., Schulz, K. G., and Riebesell, U.: Influence of plankton community structure on the sinking velocity of marine aggregates, Global Biogeochem Cycles, 30, 1145–1165, https://doi.org/10.1029/2019GB006256, 2016.

Bach, L. T., Gill, S. J., Rickaby, R. E. M., Gore, S., and Renforth, P.: CO2 Removal With Enhanced Weathering and Ocean
440 Alkalinity Enhancement, Frontiers in Climate, 1:7, https://doi.org/10.3389/fclim.2019.00007, 2019a.

Bach, L. T., Hernández-Hernández, N., Taucher, J., Spisla, C., Sforna, C., Riebesell, U., and Arístegui, J.: Effects of Elevated CO2 on a Natural Diatom Community in the Subtropical NE Atlantic, Front Mar Sci, 6:75, 320, https://doi.org/10.3389/fmars.2019.00075, 2019b.

Bach, L. T., Stange, P., Taucher, J., Achterberg, E. P., Algueró-Muñiz, M., Horn, H., Esposito, M., and Riebesell, U.: The
445 Influence of Plankton Community Structure on Sinking Velocity and Remineralization Rate of Marine Aggregates, Global Biogeochem Cycles, 33, 971–994, https://doi.org/10.1029/2019GB006256, 2019c.

Bach, L. T., Paul, A. J., Boxhammer, T., Esch, E., Graco, M., Schulz, K. G., Achterberg, E., Aguayo, P., Ar\'ıstegui, J., Ayón, P., Baños, I., Bernales, A., Boegeholz, A. S., Chavez, F., Chavez, G., Chen, S.-M., Doering, K., Filella, A., Fischer, M., Grasse, P., Haunost, M., Hennke, J., Hernández-Hernández, N., Hopwood, M., Igarza, M., Kalter, V., Kittu, L., Kohnert, P., Ledesma,
450 J., Lieberum, C., Lischka, S., Löscher, C., Ludwig, A., Mendoza, U., Meyer, J., Minutolo, F., Ortiz Cortes, J., Piiparinen, J., Sforna, C., Spilling, K., Sanchez, S., Spisla, C., Sswat, M., Zavala Moreira, M., and Riebesell, U.: Factors controlling plankton community production, export flux, and particulate matter stoichiometry in the coastal upwelling system off Peru, Biogeosciences, 17, 4831–4852, https://doi.org/10.5194/bg-17-4831-2020, 2020.

Böckmann, S., Koch, F., Meyer, B., Pausch, F., Iversen, M., Driscoll, R., Laglera, L. M., Hassler, C., and Trimborn, S.: Salp
455 fecal pellets release more bioavailable iron to Southern Ocean phytoplankton than krill fecal pellets, Current Biology, 31, 2737-2746.e3, https://doi.org/10.1016/j.cub.2021.02.033, 2021.

Bopp, L., Resplandy, L., Orr, J. C., Doney, S. C., Dunne, J. P., Gehlen, M., Halloran, P., Heinze, C., Ilyina, T., and Seferian, R.: Multiple stressors of ocean ecosystems in the 21st century, Biogeosciences, 10, 6225–6245, https://doi.org/10.5194/bg-10-6225-2013, 2013.

460 Boxhammer, T., Bach, L. T., Czerny, J., and Riebesell, U.: Technical note: Sampling and processing of mesocosm sediment trap material for quantitative biogeochemical analysis, Biogeosciences, 13, 2849–2858, https://doi.org/10.5194/bg-13-2849-2016, 2016.

Boyd, P. W., Sherry, N. D., Berges, J. A., Bishop, J. K. B., Calvert, S. E., Charette, M. A., Giovannoni, S. J., Goldblatt, R., Harrison, P. J., Moran, S. B., Roy, S., Soon, M., Strom, S., Thibault, D., Vergin, K. L., Whitney, F. A., and Wong, C. S.: Transformations of biogenic particulates from the pelagic to the deep ocean realm, Deep Sea Research Part II: Topical Studies in Oceanography, 46, 2761–2792, https://doi.org/10.1016/S0967-0645(99)00083-1, 1999.

Brečević, L. and Nielsen, A. E.: Solubility of amorphous calcium carbonate, J Cryst Growth, 98, 504–510, https://doi.org/10.1016/0022-0248(89)90168-1, 1989.

Byrne, C. D., Law, R. J., Hudson, P. M., Thain, J. E., and Fileman, T. W.: Measurements of the dispersion of liquid industrial waste discharged into the wake of a dumping vessel, Water Res, 22, 1577–1584, https://doi.org/10.1016/0043-1354(88)90171-6, 1988.

Cabanes, D. J. E., Norman, L., Santos-Echeandía, J., Iversen, M. H., Trimborn, S., Laglera, L. M., and Hassler, C. S.: First Evaluation of the Role of Salp Fecal Pellets on Iron Biogeochemistry, Front Mar Sci, 3, https://doi.org/10.3389/fmars.2016.00289, 2017.

Cherabier, P. and Ferrière, R.: Eco-evolutionary responses of the microbial loop to surface ocean warming and consequences for primary production, ISME J, 16, 1130–1139, https://doi.org/10.1038/s41396-021-01166-8, 2022.

Ciais, P., Sabine, C., Bala, G., Bopp, L., Brovkin, V., Canadell, J., Chhabra, A., DeFries, R., Galloway, J., and Heimann, M.: Carbon and Other Biogeochemical Cycles, in: Climate Change 2013 – The Physical Science Basis: Working Group I Contribution to the Fifth Assessment Report of the Intergovernmental Panel on Climate Change, edited by: Change, I. P. on C., Cambridge University Press, Cambridge, 465–570, https://doi.org/10.1017/CBO9781107415324.015, 2014.

Coverly, S., Kérouel, R., and Aminot, A.: A re-examination of matrix effects in the segmented-flow analysis of nutrients in sea and estuarine water, Anal Chim Acta, 712, 94–100, https://doi.org/10.1016/j.aca.2011.11.008, 2012.

Dickson, A.: Standards for Ocean Measurements, Oceanography, 23, 34–47, https://doi.org/10.5670/oceanog.2010.22, 2010.

Doney, S. C., Fabry, V. J., Feely, R. A., and Kleypas, J. A.: Ocean Acidification, Ann Rev Mar Sci, 1, 169–192, https://doi.org/10.1146/annurev.marine.010908.163834, 2009.

Endres, S., Galgani, L., Riebesell, U., Schulz, K.-G., and Engel, A.: Stimulated Bacterial Growth under Elevated pCO2: Results from an Off-Shore Mesocosm Study, PLoS One, 9, e99228-, 2014.

Engel, A., Abramson, L., Szlosek, J., Liu, Z., Stewart, G., Hirschberg, D., and Lee, C.: Investigating the effect of ballasting by CaCO3 in Emiliania huxleyi, II, Deep Sea Research Part II: Topical Studies in Oceanography, 56, 1408–1419, https://doi.org/10.1016/j.dsr2.2008.11.028, 2009.

Feng, E. Y., Koeve, W., Keller, D. P., and Oschlies, A.: Model-Based Assessment of the CO2 Sequestration Potential of Coastal Ocean Alkalinization, Earths Future, 5, 1252–1266, https://doi.org/10.1002/2017EF000659, 2017.

Ferderer, A., Chase, Z., Kennedy, F., Schulz, K. G., and Bach, L. T.: Assessing the influence of ocean alkalinity enhancement on a coastal phytoplankton community, Biogeosciences, 19, 5375–5399, https://doi.org/10.5194/bg-19-5375-2022, 2022.

Francois, R., Honjo, S., Krishfield, R., and Manganini, S.: Factors controlling the flux of organic carbon to the bathypelagic zone of the ocean, Global Biogeochem Cycles, 16, 34-1-34–20, https://doi.org/10.1029/2001GB001722, 2002.

Gattuso, J.-P., Magnan, A., Billé, R., Cheung, W. W. L., Howes, E. L., Joos, F., Allemand, D., Bopp, L., Cooley, S. R., Eakin, C. M., Hoegh-Guldberg, O., Kelly, R. P., Pörtner, H.-O., Rogers, A. D., Baxter, J. M., Laffoley, D., Osborn, D., Rankovic, A., Rochette, J., Sumaila, U. R., Treyer, S., and Turley, C.: Contrasting futures for ocean and society from different anthropogenic CO2 emissions scenarios, Science (1979), 349, https://doi.org/10.1126/science.aac4722, 2015.

GESAMP: High level review of a wide range of proposed marine geoengineering techniques, 98th ed., edited by: GESAMP, International Maritime Organization, London, 2019.

González, M. F. and Ilyina, T.: Impacts of artificial ocean alkalinization on the carbon cycle and climate in Earth system simulations, Geophys Res Lett, 43, 6493–6502, https://doi.org/10.1002/2016GL068576, 2016.

Griffioen, J.: Enhanced weathering of olivine in seawater: the efficiency as revealed by thermodynamic scenario analysis, Science of the Total Environment, 575, 536–544, https://doi.org/10.1016/j.scitotenv.2016.09.008, 2017.

Guidi, L., Legendre, L., Reygondeau, G., Uitz, J., Stemmann, L., and Henson, S. A.: A new look at ocean carbon remineralization for estimating deepwater sequestration, Global Biogeochem Cycles, 29, 1044–1059, https://doi.org/10.1002/2014GB005063, 2015.

Hansen, H. P. and Koroleff, F.: Determination of nutrients, in: Methods of Seawater Analysis, 159–228, https://doi.org/10.1002/9783527613984.ch10, 1999.

Hartmann, J., West, A. J., Renforth, P., Köhler, P., La Rocha, C. L., Wolf-Gladrow, D. A., Dürr, H. H., and Scheffran, J.: Enhanced chemical weathering as a geoengineering strategy to reduce atmospheric carbon dioxide, supply nutrients, and mitigate ocean acidification, Reviews of Geophysics, 51, 113–149, https://doi.org/10.1002/rog.20004, 2013.

Hartmann, J., Suitner, N., Lim, C., Schneider, J., Mar\'{\i}n-Samper, L., Ar\'{\i}stegui, J., Renforth, P., Taucher, J., and Riebesell, U.: Stability of alkalinity in ocean alkalinity enhancement (OAE) approaches – consequences for durability of CO2 storage, Biogeosciences, 20, 781–802, https://doi.org/10.5194/bg-20-781-2023, 2023.

Hessen, D. O., Ågren, G. I., Anderson, T. R., Elser, J. J., and De Ruiter, P. C.: Carbon sequestration in ecosystems: the role of stoichiometry, Ecology, 85, 1179–1192, https://doi.org/10.1890/02-0251, 2004.

Honjo, S., Manganini, S. J., Krishfield, R. A., and Francois, R.: Particulate organic carbon fluxes to the ocean interior and factors controlling the biological pump, Prog Oceanogr, 76, 217–285, https://doi.org/10.1016/j.pocean.2007.11.003, 2008.

Iversen, M. H.: Carbon Export in the Ocean: A Biologist's Perspective, Ann Rev Mar Sci, 15, 357–381, https://doi.org/10.1146/annurev-marine-032122-035153, 2023.

Iversen, M. H. and Ploug, H.: Temperature effects on carbon-specific respiration rate and sinking velocity of diatom aggregates-potential implications for deep ocean export processes, Biogeosciences, 10, 4073–4085, https://doi.org/10.5194/bg-10-4073-2013, 2013.

Jokiel, P. L.: The reef coral two compartment proton flux model, J Exp Mar Biol Ecol, 409, 1–12, https://doi.org/10.1016/j.jembe.2011.10.008, 2011.

Jordan, R. W.: Coccolithophores, in: Encyclopedia of Microbiology (Third Edition), edited by: Schaechter, M., Academic Press, Oxford, 593–605, https://doi.org/10.1016/B978-012373944-5.00249-2, 2009.

Karthäuser, C., Ahmerkamp, S., Marchant, H. K., Bristow, L. A., Hauss, H., Iversen, M. H., Kiko, R., Maerz, J., Lavik, G., and Kuypers, M. M. M.: Small sinking particles control anammox rates in the Peruvian oxygen minimum zone, Nat Commun, 12, 3235, https://doi.org/10.1038/s41467-021-23340-4, 2021.

Kheshgi, H. S.: Sequestering atmospheric carbon dioxide by increasing ocean alkalinity, Energy, 20, 915–922, 535 https://doi.org/10.1016/0360-5442(95)00035-F, 1995.

Klaas, C. and Archer, D. E.: Association of sinking organic matter with various types of mineral ballast in the deep sea, Global Biogeochem Cycles, 16, 63-1-63–14, https://doi.org/10.1029/2001GB001765, 2002.

Koeve, W.: Upper ocean carbon fluxes in the Atlantic Ocean, Global Biogeochem Cycles, 16, 4-1-4–17, https://doi.org/10.1029/2001GB001836, 2002.

540 Köhler, P., Hartmann, J., and Wolf-Gladow, D. A.: Geoengineering potential of artificially enhanced silicate weathering of olivine, Proceedings of the National Academy of Sciences, 107, 20228–20233, https://doi.org/10.1073/pnas.1000545107, 2010.

Kwon, E. Y., Primeau, F., and Sarmiento, J. L.: The impact of remineralization depth on the air–sea carbon balance, Nat Geosci, 2, 630–635, https://doi.org/10.1038/ngeo612, 2009.

545 Li, C., Luo, X., Huang, X., and Gu, B.: Effects of Temperature, Salinity, pH, and Light on Filtering and Grazing Rates of a Calanoid Copepod (Schmackeria dubia), ScientificWorldJournal, 8, 838071, https://doi.org/10.1100/tsw.2008.153, 2008.

Lüdecke, D., Ben-Shachar, M., Patil, I., Waggoner, P., and Makowski, D.: performance, J Open Source Softw, 6, 3139, https://doi.org/10.21105/joss.03139, 2021.

Lueker, T. J., Dickson, A. G., and Keeling, C. D.: Ocean pCO2 calculated from dissolved inorganic carbon, alkalinity, and 550 equations for K1 and K2, Mar Chem, 70, 105–119, https://doi.org/10.1016/S0304-4203(00)00022-0, 2000.

Martínez-García, A., Sigman, D. M., Ren, H., Anderson, R. F., Straub, M., Hodell, D. A., Jaccard, S. L., Eglinton, T. I., and Haug, G. H.: Iron fertilization of the Subantarctic Ocean during the last ice age, Science (1979), 343, 1347–1350, https://doi.org/10.1126/science.1246848, 2014.

Masson-Delmotte, V., Zhai, P., Pörtner, H.-O., Roberts, D., Skea, J., Shukla, P. R., al., et, and IPCC (Eds.): Climate Change 555 2021: The Physical Science Basis., Cambridge University Press, 2021.

McCave, I. N.: Particulate size spectra, behavior, and origin of nepheloid layers over the Nova Scotian Continental Rise, J Geophys Res Oceans, 88, 7647–7666, https://doi.org/10.1029/JC088iC12p07647, 1983.

Le Moigne, F. A. C., Henson, S. A., Cavan, E., Georges, C., Pabortsava, K., Achterberg, E. P., Ceballos-Romero, E., Zubkov, M., and Sanders, R. J.: What causes the inverse relationship between primary production and export efficiency in the Southern 560 Ocean?, Geophys Res Lett, 43, 4457–4466, https://doi.org/10.1002/2016GL068480, 2016.

Monteiro, F., Bach, L. T., Brownlee, C., Bown, P., E, R. R., Poulton, A. J., Tyrrell, T., Beaufort, L., Dutkiewicz, S., Gibbs, S., Gutowska, M. A., Lee, R., Riebesell, U., Young, J., and Ridgwell, A.: Why marine phytoplankton calcify, Sci Adv, 2, e1501822, https://doi.org/10.1126/sciadv.1501822, 2016.

Moras, C. A., Bach, L. T., Cyronak, T., Joannes-Boyau, R., and Schulz, K. G.: Ocean Alkalinity Enhancement - Avoiding
565   runaway CaCO₃ precipitation during quick and hydrated lime dissolution, Biogeosciences Discussions, 1–31,
https://doi.org/10.5194/bg-2021-330, 2021.

Moras, C. A., Bach, L. T., Cyronak, T., Joannes-Boyau, R., and Schulz, K. G.: Ocean alkalinity enhancement - avoiding
runaway CaCO3 precipitation during quick and hydrated lime dissolution, Biogeosciences, 19, 3537–3557,
https://doi.org/10.5194/bg-19-3537-2022, 2022.

570   Morris, A. W. and Riley, J. P.: The determination of nitrate in sea water, Anal Chim Acta, 29, 272–279,
https://doi.org/10.1016/S0003-2670(00)88614-6, 1963.

Morse, J. W. and He, S.: Influences of T, S and PCO2 on the pseudo-homogeneous precipitation of CaCO3 from seawater,
Mar Chem, 41, 291–297, https://doi.org/10.1016/0304-4203(93)90261-L, 1993.

Mucci, A.: The solubility of calcite and aragonite in seawater at various salinities, temperatures, and one atmosphere total
575   pressure, Am. J. Sci, 283, 780–799, 1983.

Mullin, J. B. and Riley, J. P.: The colorimetric determination of silicate with special reference to sea and natural waters, Anal
Chim Acta, 12, 162–176, https://doi.org/10.1016/S0003-2670(00)87825-3, 1955.

Murphy, J. and Riley, J. P.: A modified single solution method for the determination of phosphate in natural waters, Anal
Chim Acta, 27, 31–36, https://doi.org/10.1016/S0003-2670(00)88444-5, 1962.

580   Paquay, F. S. and Zeebe, R. E.: Assessing possible consequences of ocean liming on ocean pH, atmospheric CO2 concentration
and   associated   costs,   International   Journal   of   Greenhouse   Gas   Control,   17,   183–188,
https://doi.org/10.1016/j.ijggc.2013.05.005, 2013.

Passow, U. and Carlson, C. A.: The biological pump in a high CO2 world, Mar Ecol Prog Ser, 470, 249–271,
https://doi.org/10.3354/meps09985, 2012.

585   Pierrot, D. E., Wallace, D. W. R., and Lewis, E.: MS Excel Program Developed for CO2 System Calculations, Oak Ridge
National Laboratory, Oak Ridge, Tennesse, https://doi.org/10.3334/CDIAC/otg.CO2SYS_XLS_CDIAC105a, 2011.

Pinheiro, J., Bates, D., DebRoy, S., Sarkar, D., and Team, R. C.: nlme: Linear and Nonlinear Mixed Effects Models, 2020.

Piontek, J., Lunau, M., Händel, N., Borchard, C., Wurst, M., and Engel, A.: Acidification increases microbial polysaccharide
degradation in the ocean, Biogeosciences, 7, 1615–1624, https://doi.org/10.5194/bg-7-1615-2010, 2010.

590   Ploug, H. and Grossart, H.-P.: Bacterial growth and grazing on diatom aggregates, Limnol Oceanogr, 45, 1467–1475,
https://doi.org/10.4319/lo.2000.45.7.1467, 2000.

Puig, P., Madron, X. D. de, Salat, J., Schroeder, K., Martín, J., Karageorgis, A. P., Palanques, A., Roullier, F., Lopez-Jurado,
J. L., Emelianov, M., Moutin, T., and Houpert, L.: Thick bottom nepheloid layers in the western Mediterranean generated by
deep dense shelf water cascading, Prog Oceanogr, 111, 1–23, https://doi.org/10.1016/j.pocean.2012.10.003, 2013.

595   Renforth, P. and Henderson, G.: Assessing ocean alkalinity for carbon sequestration, Reviews of Geophysics, 55, 636–674,
https://doi.org/10.1002/2016RG000533, 2017.

Riebesell, U., Wolf-Gladrow, D. A., and Smetacek, V.: Carbon dioxide limitation of marine phytoplankton growth rates, Nature, 361, 249–251, https://doi.org/10.1038/361249a0, 1993.

Riebesell, U., Bach, L. T., Bellerby, R. G. J., Monsalve, J., Boxhammer, T., Czerny, J., Larsen, A., Ludwig, A., and Schulz,
600   K. G.: Competitive fitness of a predominant pelagic calcifier impaired by ocean acidification, Nat Geosci, 10, 19–23, https://doi.org/10.1038/ngeo2854, 2017.

Ristow, G. H.: Wall correction factor for sinking cylinders in fluids, Phys Rev E, 55, 2808–2813, https://doi.org/10.1103/PhysRevE.55.2808, 1997.

Rodriguez-Blanco, J. D., Sand, K. K., and Benning, L. G.: ACC and Vaterite as Intermediates in the Solution-Based
605   Crystallization of CaCO3, in: New Perspectives on Mineral Nucleation and Growth: From Solution Precursors to Solid Materials, edited by: van Driessche, A. E. S., Kellermeier, M., Benning, L. G., and Gebauer, D., Springer International Publishing, Cham, 93–111, https://doi.org/10.1007/978-3-319-45669-0_5, 2017.

Rothwell, R. G.: Sedimentary Rocks, in: Reference Module in Earth Systems and Environmental Sciences, Elsevier, https://doi.org/10.1016/B978-0-12-409548-9.10493-2, 2016.

610   Salter, I., Schiebel, R., Ziveri, P., Movellan, A., Lampitt, R., and Wolff, G. A.: Carbonate counter pump stimulated by natural iron fertilization in the Polar Frontal Zone, Nat Geosci, 7, 885–889, https://doi.org/10.1038/ngeo2285, 2014.

Sarthou, G., Vincent, D., Christaki, U., Obernosterer, I., Timmermans, K. R., and Brussaard, C. P. D.: The fate of biogenic iron during a phytoplankton bloom induced by natural fertilisation: Impact of copepod grazing, Deep Sea Research Part II: Topical Studies in Oceanography, 55, 734–751, https://doi.org/10.1016/j.dsr2.2007.12.033, 2008.

615   Schmittner, A., Oschlies, A., Schulz, K. G., and Riebesell, U.: Simulated 21st century's increase in oceanic suboxia by CO2-enhanced biotic carbon export, Global Biogeochem Cycles, 22, GB4008, https://doi.org/10.1029/2007GB003147, 2008.

Schneider, B., Schlitzer, R., Fischer, G., and Nöthig, E.-M.: Depth-dependent elemental compositions of particulate organic matter (POM) in the ocean, Global Biogeochem Cycles, 17, https://doi.org/10.1029/2002GB001871, 2003.

Shaffer, G.: Biogeochemical cycling in the global ocean, J Geophys Res Oceans, 101, 3723–3745,
620   https://doi.org/10.1029/95JC03373, 1996.

Sharp, J. H.: Improved analysis for "particulate" organic carbon and nitrogen from seawater, Limnol Oceanogr, 19, 984–989, https://doi.org/10.4319/lo.1974.19.6.0984, 1974.

Smith, P., Davis, S. J., Creutzig, F., Fuss, S., Minx, J., Gabrielle, B., Kato, E., Jackson, R. B., Cowie, A., and Kriegler, E.: Biophysical and economic limits to negative CO2 emissions, Nat Clim Chang, 6, 42–50, https://doi.org/10.1038/nclimate2870,
625   2016.

S, N. A.: A Research Strategy for Ocean-based Carbon Dioxide Removal and Sequestration, National Academies Press, Washington, D.C., https://doi.org/10.17226/26278, 2021.

Stange, P., Taucher, J., Bach, L. T., Algueró-Muñiz, M., Horn, H. G., Krebs, L., Boxhammer, T., Nauendorf, A. K., and Riebesell, U.: Ocean Acidification-Induced Restructuring of the Plankton Food Web Can Influence the Degradation of Sinking
630   Particles, Front Mar Sci, 5, https://doi.org/10.3389/fmars.2018.00140, 2018.

Strickland, J. D. H. and Parsons, T. R.: A practical handbook of seawater analysis, 2. ed., Bulletin (Fisheries Research Board of Canada), Ottawa, 1972.

Stukel, M. R., Landry, M. R., Benitez-Nelson, C. R., and Goericke, R.: Trophic cycling and carbon export relationships in the California Current Ecosystem, Limnol Oceanogr, 56, 1866–1878, https://doi.org/10.4319/lo.2011.56.5.1866, 2011.

635 Subhas, A. V, Marx, L., Reynolds, S., Flohr, A., Mawji, E. W., Brown, P. J., and Cael, B. B.: Microbial ecosystem responses to alkalinity enhancement in the North Atlantic Subtropical Gyre, Frontiers in Climate, 4, https://doi.org/10.3389/fclim.2022.784997, 2022.

Taucher, J. and Oschlies, A.: Can we predict the direction of marine primary production change under global warming?, Geophys Res Lett, 38, LO2603, https://doi.org/10.1029/2010GL045934, 2011.

640 Taucher, J., Bach, L. T., Boxhammer, T., Nauendorf, A., Consortium, T. G. C. K., Achterberg, E. P., Algueró-Muñiz, M., Arístegui, J., Czerny, J., Esposito, M., Guan, W., Haunost, M., Horn, H. G., Ludwig, A., Meyer, J., Spisla, C., Sswat, M., Stange, P., and Riebesell, U.: Influence of Ocean Acidification and Deep Water Upwelling on Oligotrophic Plankton Communities in the Subtropical North Atlantic, Front Mar Sci, 4, https://doi.org/10.3389/fmars.2017.00085, 2017.

Taucher, J., Boxhammer, T., Bach, L. T., Paul, A. J., Schartau, M., Stange, P., and Riebesell, U.: Changing carbon-to-nitrogen
645 ratios of organic-matter export under ocean acidification, Nat Clim Chang, 11, 52–57, https://doi.org/10.1038/s41558-020-00915-5, 2021.

Taylor, L. L., Quirk, J., Thorley, R. M. S., Kharecha, P. A., Hansen, J., Ridgwell, A., Lomas, M. R., Banwart, S. A., and Beerling, D. J.: Enhanced weathering strategies for stabilizing climate and averting ocean acidification, Nat Clim Chang, 6, 402–406, https://doi.org/10.1038/nclimate2882, 2016.

650 Team, R. C.: R: A language and environment for statistical computing., R Foundation for Statistical Computing, Vienna, Austria, 2021.

Webb, A. L., Malin, G., Hopkins, F. E., Ho, K. L., Riebesell, U., Schulz, K., Larsen, A., and Liss, P.: Ocean acidification affects production of DMS and DMSP measured in a mesocosm study and cultures of Emiliania huxleyi and a mesocosm study:, Environ. Chem, 13, 314–329, https://doi.org/10.1071/EN14268, 2016.

655 Welschmeyer, N. A.: Fluorometric analysis of chlorophyll a in the presence of chlorophyll b and pheopigments, Limnol Oceanogr, 39, 1985–1992, https://doi.org/10.4319/lo.1994.39.8.1985, 1994.

Wickham, H., Averick, M., Bryan, J., Chang, W., McGowan, L., François, R., Grolemund, G., Hayes, A., Henry, L., Hester, J., Kuhn, M., Pedersen, T., Miller, E., Bache, S., Müller, K., Ooms, J., Robinson, D., Seidel, D., Spinu, V., Takahashi, K., Vaughan, D., Wilke, C., Woo, K., and Yutani, H.: Welcome to the Tidyverse, J Open Source Softw, 4, 1686,
660 https://doi.org/10.21105/joss.01686, 2019.

Wurgaft, E., Wang, Z. A., Churchill, J. H., Dellapenna, T., Song, S., Du, J., Ringham, M. C., Rivlin, T., and Lazar, B.: Particle Triggered Reactions as an Important Mechanism of Alkalinity and Inorganic Carbon Removal in River Plumes, Geophys Res Lett, 48, e2021GL093178, https://doi.org/10.1029/2021GL093178, 2021.

Zagarese, H. E., Sagrario, M. de los Á. G., Wolf-Gladrow, D., Nõges, P., Nõges, T., Kangur, K., Matsuzaki, S.-I. S., Kohzu,
665   A., Vanni, M. J., Özkundakci, D., Echaniz, S. A., Vignatti, A., Grosman, F., Sanzano, P., Van Dam, B., and Knoll, L. B.:
Patterns of CO2 concentration and inorganic carbon limitation of phytoplankton biomass in agriculturally eutrophic lakes,
Water Res, 190, 116715, https://doi.org/10.1016/j.watres.2020.116715, 2021.

Zeebe, R. E. and Wolf-Gladrow, D. A.: CO2 in seawater: Equilibrium, kinetics, isotopes, edited by: Zeebe, R. E. and Wolf-
Gladrow, D. A., Elsevier, Amsterdam; New York, 346 pp., 2010.

670